Springer

KSME

Journal of Mechanical Science and Technology 26 (8) (2012) 2337~2345
www.springerlink.com/content/1738-494x
DOI 10.1007/s12206-012-0617-y

Pyramid as test geometry to evaluate formability in incremental forming: Recent results †

Ghulam Hussain*, Nasir Hayat and Gao Lin

College of Electrical and Mechanical Engineering, Nanjing University of Aeronautics & Astronautics, Nanjing, 210016, China

(Manuscript Received June 2, 2011; Revised March 12, 2012; Accepted March 28, 2012)

Abstract

The present work has been undertaken with an objective to fill the gaps of previous studies and to explore guidelines to standardize the test specimen for evaluating formability with a single specimen in single point incremental forming (SPIF). Two candidate geometries for formability testing (i.e. varying wall angle pyramidal frustum and varying wall angle conical frustum) have been compared by varying geometrical parameters and materials. The critical size in horizontal plane (i.e. half-side length/curvature radius) and critical initial forming angle have been identified and compared for the two geometries. The critical size in horizontal plane has been found to be different for the two geometries. The critical initial forming angle has been found to be same for the two geometries. For various sheet materials, the difference in the formability of VWACF and VWAPF shows a dependence upon the percent reduction in area at tensile fracture.

Keywords: Formability; Geometry; Incremental forming; Parameter; Standardization; Test

1. Introduction

In the last decade, several new manufacturing processes, such as hydro-forming [1-3], laser forming [4], water jet forming [5], dimple forming [6], flexible hull forming [7] and incremental forming [8], have been introduced. However, owing to high flexibility and low tooling cost, single point incremental forming (SPIF) has attained a great attention in industrial sector. The SPIF process can perform 3-D shaping without dedicated dies. But the process, due to slow forming speed, is feasible for small batch size. The process has found several applications in automotive [9, 10] and biomedical sectors [11]. The process is also useful for waste sheet recycling [12]. Further, it is capable to process polymers [13] besides sheet metal.

In the simplest form of SPIF, the sheet is clamped on a rig and a hemispherical end tool, made of steel rod, incrementally steps down the sheet to form desired contour. The tool motion is controlled through a pre-defined trajectory. For further process details and advances made so far, the reader is referred to Ref. [8].

In SPIF, the deformation imposed by the tool on the sheet is confined to the processing zone only and is combination of stretching and shearing [14]. As a result of this peculiar deformation mechanism, sheet thinning occurs during SPIF. The final wall thickness (i.e. after thinning) becomes less than that of the original blank sheet and, especially under uni-axial deformation, can be approximated by the Sine law. Mathematically, the law is expressed as follows:

$$t_f = t_o Sin\,(90-\theta) \tag{1}$$

where t_f is the final wall thickness, t_o is the blank thickness and θ is the wall angle. According to the above equation, the wall thinning mainly depends upon the wall angle imposed. Further the sheet fracture will occur somewhere between 0^o and 90^o. Therefore, as agreed upon by the researchers [8], the formability in SPIF is defined as the maximum value of wall angle (i.e. θ_{max}) without sheet fracture.

Though wall angle is the principal factor affecting wall thinning in SPIF, part curvature and initial forming angle imposed could also contribute to sheet thinning. Small curvature radii promote biaxial deformation (i.e. $\varepsilon_2 \neq 0$) [15, 16], and large values of initial forming angle induce thinning band in sheet (thinning band is an excessively thinned, higher than the sine law's prediction, segment of part located in the flange area) [17]. Both biaxial deformation and thinning band induce undue thinning, higher than the sine law's prediction, in sheet [15-17]. As a consequence, the sheet achieves its thinning limit at a smaller wall angle and hence the formability (i.e. θ_{max}) reduces.

Cone and pyramid, being simple, are two potential geometries for determining formability (i.e. θ_{max}) in SPIF. Shim and

*Corresponding author. Tel.: +86 13675161625, Fax.: +86 25 84896469
E-mail address: gh_ghumman@yahoo.com
† Recommended by Associate Editor Youngseog Lee

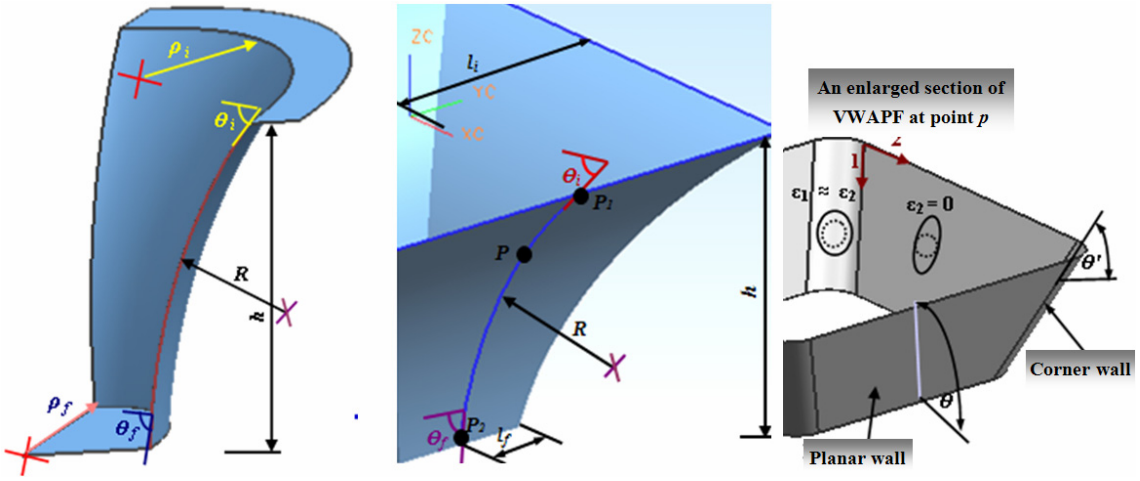

(a) VWACF (b) VWAPF

Fig. 1. Test geometries with wall angle continuously varying along the depth and geometrical parameters: (a) Frustum of cone; (b) Frustum of pyramid.

Park [15] and Capece et al. [18] have reported that the cone acquires higher formability than the pyramid. The authors in their investigations did not take into account the influence of variation in geometrical parameters, especially those of pyramid, upon formability. Therefore, the conclusion regarding the comparative formability of cone and pyramid cannot be generalized without further investigating the effect of geometrical parameters on formability in a systematic way.

Several studies with emphasis on formability in SPIF have been reported in literature [15-21]. The shape and size of test specimen have not been standardized so far, however. In fact, the knowledge in a quantified form on various aspects of test geometry (i.e. effect of variation in size and shape on formability) is not available to a sufficient level. The aforementioned geometrical aspects need to be adequately addressed in order to reach to conclusive results. Hussain and co-workers [16, 17, 19] have partially studied the above aspects. They have examined the effect of variation in the size (i.e. geometrical parameters) of test geometry on formability. Only one test geometry (i.e. a frustum of cone with varying wall angle abbreviated as VWACF and shown in Fig. 1(a) was investigated, however. In this paper, the other potential test geometry (i.e. pyramid), with an aim to analyze the effect of variation in shape on formability, is brought under study. A frustum of pyramid with wall angle continuously varying along the depth (abbreviated as VWAPF and shown in Fig. 1(b)) is employed as the test geometry. The important geometrical parameters of the pyramidal frustum are varied over wide ranges and their effect upon the formability (i.e. θ_{max}) is quantified. The results of the newly investigated geometry (i.e. VWAPF) are compared with those of the previously investigated one (i.e. VWACF). Furthermore, a comparison between the formability of two geometries at varying sheet material is also drawn. As a result of this study, it has become possible to standardize the test specimen to test formability in SPIF.

2. Details of test geometry

Figs. 1(a) and 1(b) show two test geometries, named as varying wall angle conical frustum (i.e. VWACF used in [16, 17, 19]) and varying wall angle pyramidal frustum (i.e. VWAPF employed in the current work) with their respective geometrical parameters. The wall angle in both the geometries continuously increases along the depth (from 0^o to 90^o), thus inducing corresponding wall thinning in the specimen. The fracture occurs somewhere between point P_1 and point P_2 (i.e. between 0^o and 90^o) whenever the thinning limit of sheet is surpassed.

Each of the shown geometries has four geometrical parameters. Three parameters, with respect to definition as well as terminology, are common in the two geometries. These are: initial forming/wall angle (θ_i), generatrix radius (R) and depth (h). However, one parameter (i.e. size in horizontal plane) differs in terminology. This parameter is termed as horizontal curvature radius (ρ_z) for VWACF and half-side length (L_z) for VWAPF. The subscript z indicates that the dimension varies along Z-axis (or depth). The preliminary study showed that the effect of variation in generatrix radius (i.e. R), in nature and quantity, on the formability of VWAPF is same as that reported in Ref. [19] for VWACF. Therefore, this parameter was not further investigated in this study. Depth of specimen varies if the initial forming angle is changed. Therefore, this parameter, being dependent on the other parameter, was also dropped out from the test plan.

Consider an arbitrary point (say P) on the two geometries. For VWACF, the wall angle corresponding to this point remains constant along the directrix. However, for VWAPF, the wall angle subtended by the planar side is larger than that subtended by the corner, as shown in an enlarged view of an arbitrary section (Fig. 1(a)). The wall angle of corner obeys

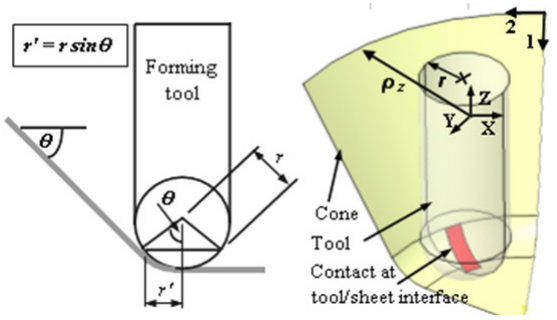

Fig. 2. Geometry of contact at the tool/sheet interface in SPIF.

the following relation:

$$\theta' = \tan^{-1}[(\sqrt{2}/2)\tan\theta] \quad (2)$$

where θ and θ' are the wall angles subtended by the planar side and corner, respectively. This variation in wall angle along with quantity of hoop strains, coming from the curvature of corner, determines the location of fracture in a pyramid. According to Ref. [18], the interface of planar side and corner experiences the maximum deformation and, therefore, the fracture in VWAPF occurs at the interfacial zone. However, this point will be further examined in the present study.

3. Contact radius of tool

Contact geometry at the tool/sheet interface in SPIF is shown in Fig. 2. As can be seen, only a fraction of tool radius makes contact with the sheet. This radius fraction increases as the wall angle increases. The fraction of tool radius staying in contact with the sheet can be termed as contact radius and can be mathematically determined from the following relation:

$$r' = r \times Sin\theta \quad (3)$$

where r and r' are the manufactured radius and contact radius of tool, respectively, and θ is the wall angle of forming geometry. The above relation shows that, if r is kept constant, there is an increase in the tool/sheet contact with an increase in the wall angle. However, the type of contact (i.e. along longitudinal/hoop direction) mainly depends upon the curvature of forming geometry: the contact will be longitudinal for large curvature radii and mixed (i.e. both along longitudinal and hoop directions) for small curvature radii [15]. These variations in the interfacial contact will in turn decide the amount of strain induced along with its type (i.e. uni-axial or bi-axial) during sheet forming. Bi-axial strains develop when the forming is performed under mixed contact.

4. Blank stiffness

In SPIF, blank stiffness is the resistance of blank to point load exerted by the tool in a direction normal to the blank plane [20]. In SPIF, blank is clamped on a hollow die. Therefore, the forming tool, while traversing over the blank, encounters the maximum stiffness near the clamped edge and the minimum at the center of blank. Moreover, the stiffness increases with the decreasing of part (or blank) size [20]. Due to these variations, the sheet while forming undergoes different amount of elastic deformations at different locations. The elastic deformation will affect tool/sheet contact in such a way that with the same forming parameters a small blank will endure higher strain than a large blank. This could lead to sheet fracture at a smaller value of θ_{max}, hence causing reduction in formability. The reader is referred to Ref. [21] for detail on blank stiffness.

Table 1. Geometrical parameters and their levels employed in the current investigations.

Variable parameter	Levels	Fixed geometrical parameters
L_i (mm)	34, 38, 40, 43, 47.8, 55.4, 65, 80, 95	$\theta_i = 43.8^o$; $\theta_f = 75^o$; $h = 53.4$ mm; $R = 115$ mm; $L_f = 2.4$ mm-63.5 mm
θ_i (degree)	48, 51, 54, 58, 61	$L_i = 80$ mm; $\theta_f = 75^o$; $h = 47.3$ mm-25 mm; $L_f = 54.3$ mm-70 mm; $R = 115$ mm

5. Test conditions and procedures

Table 1 lists the levels over which the geometrical parameters of VWAPF (i.e. varying wall angle pyramid) were varied. These levels are the same as Hussain and co-workers in their studies [16, 17, 19] had employed for VWACF (i.e. varying wall angle cone). In order to examine the effect of variation in the size in horizontal plane on formability, the initial half-side length (i.e. L_i as defined in Fig. 1) of VWAPF was varied from 34 mm to 95 mm. As a result, its final half-side length (i.e. L_f as defined in Fig. 1) also underwent variation as shown in Table 1. The initial forming angle (i.e. θ_i) was varied from 48° to 61°. Due to this variation, the depth of specimen also underwent variation (see Table 1). The remaining parameter (i.e. generatrix radius), however, was kept constant as in Ref. [17].

The AA-2024O sheet with 1.4 mm thickness, the same as employed for VWACF [16, 17, 19], was used as the experimental material. In order to study the strain state on test specimen, grid pattern was printed on each blank specimen. All the tests were performed with the following fixed process parameters:

Feed rate (f) = 2.6 m/min; Tool radius (r) = 4 mm; Step size (p) = 0.4 mm; Lubricant = Mineral oil.

Each test specimen was formed to fracture. And, in order to provide statistical means, at least three specimens for each test were produced. In order to quantify and compare the effect of variation in geometrical parameters on sheet deformation, a point on each specimen corresponding to 66.5° wall angle (an arbitrary point of ease) was chosen as a fixed reference for strain measurement. This is clarified that the distance of this reference point from fracture point will increase (i.e. along Z direction) if the sheet forming limit (i.e. θ_{max}) increases. The

deformed grids were measured with a tool maker microscope (least count 0.001 mm) and its results were converted into true strains. In order to quantitatively analyze the effect of variation in geometrical size on wall thinning, the wall thickness in each specimen was measured from the same location as chosen for strain measurement (i.e. from a point corresponding to 66.5°). The point corresponding to 66.5° above fracture was marked and the thickness on this point was measured using a dial gauge indicator with 0.001 mm accuracy. In order to determine θ_{max}, the depth of specimen corresponding to fracture point was measured with a height gauge (least count = 0.001 mm). And the wall angle corresponding to fracture, regarded as θ_{max}, was computed adopting the procedure reported in Refs. [16, 17]. At desired depth, the curvature radius/half-side length was determined from the CAD model of respective geometry.

6. Results and discussion

In the following sub-sections, first the results pertaining to VWAPF (present study) are discussed, and later a comparison of these results with those of VWACF (previous work) is made to draw important conclusions to set guidelines in order to standardize the test geometry.

6.1 Effect of variation in half-side length

Fig. 3(a) shows the variation in wall thinning as a function of half-side length of VWAPF (half-side length was measured at the same point where thinning/strains were measured (i.e. 66.5°)). It is evident from the figure that up to half-side length of 28 mm, the wall thinning increases as the half-side length decreases. Afterwards, wall thinning remains insensitive to any variation in half-side length. Within the investigated range of half-side length, there is a variation of about 6.2% in wall thinning. Therefore, it can be said that a variation in half-side length affects the sheet deformation in SPIF. This finding can be attributed to variation in blank stiffness (refer to section 4 for details on blank stiffness). Fig. 3(a) shows the strain components at two extreme settings of half-side length. The magnitude of each component decreases with increase in half-side length. This result could only be an outcome of reduction in tool/sheet contact (which physically could not be measured due to unavailability of instruments) in hoop as well as in longitudinal directions. This clearly justifies the role of blank stiffness on sheet deformation in SPIF.

Fig. 3(a) also depicts the comparison of wall thinning, under the same testing conditions, between VWAPF and VWACF (data for VWACF adopted from Ref. [16]). The wall thinning for VWAPF has been drawn against half-side length and for VWACF has been drawn against horizontal curvature radius (an equivalent of half-side length). Both the geometries show similar trend of decrease in wall thinning with an increase in the size in horizontal plane (i.e. half-side length/horizontal curvature radius).

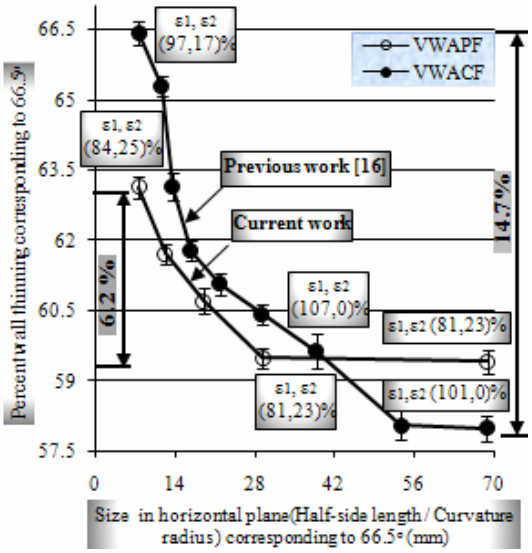

(a)

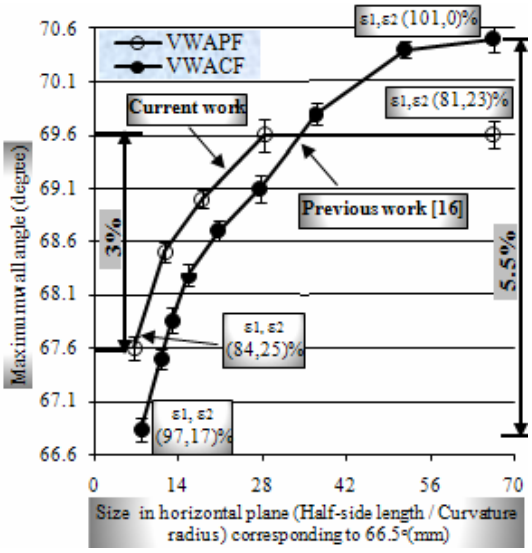

(b)

Fig. 3. Effect of variation in the size of test geometry in horizontal plane upon: (a) Wall thinning; (b) Formability.

This is to be noticed that, for the size ranging from 7 mm to 37 mm, the wall thinning of VWAPF remains lower than that of VWACF. However, after 37 mm the trend becomes reverse.

The above wall thinning trend can be attributed to the pattern of hoop strains development in the two geometries. In VWAPF, corner is the only curved feature where hoop strains can develop, and the curvature of this feature does not change as the size of VWAPF changes. Therefore, the quantity of hoop strains in VWAPF is not affected significantly as the size of VWAPF is varied. However, a slight variation (Δ = 2%) in the quantity of hoop strains (see Fig. 3(a)) owing to variation in bank stiffness can be seen. This means the major contribution towards above reported wall thinning trend is made by VWACF and this is endorsed by large variation (Δ =

17%) in hoop strains. In VWACF with curvature radius (i.e. geometry size in horizontal plane) below 37 mm, the hoop strains develop, although with decreasing quantity with increase in curvature radius (see Fig. 3(a)). Due to this fact, higher deformation occurs in VWACF than in VWAPF (compare sum of strain components at 7 mm size in Fig. 3(a)), hence inducing higher wall thinning in VWACF than in VWAPF. However, as soon as the curvature radius exceeds 37 mm, hoop strains no longer develop in VWACF (see Fig. 3(a)) and, as a result, the VWACF undergoes smaller deformation than VWAPF (compare sum of strain components at 70 mm). Consequently, lower wall thinning occurs in VWACF than in VWAPF when the size of geometry is kept above 37 mm.

The variation in wall thinning in VWAPF is about 6.2% whereas that in VWACF is about 14%. This means that the geometry size in horizontal plane is more influential upon VWACF than upon VWAPF. This is to be pointed out that the wall thinning in VWAPF (i.e. 6.2%) owes to the sole effect of varying blank stiffness, whereas that in VWACF (i.e. 14%) is due to the combined effect of varying curvature and blank stiffness.

Shim and Park [15] and Capece et al. [18] have reported that a pyramid undergoes larger deformation than a cone. The above findings clarify that the conclusion drawn in Refs. [15] and [18] is valid only for large curvature radii (i.e. above 37 mm); however, not valid for smaller curvature radii (i.e. below 37 mm). Therefore, it can be said that a pyramid does not always necessarily undergo larger deformation than a cone rather the outcome depends upon the size of test specimen in horizontal plane. The difference between the current finding and the one reported in Refs. [15] and [18] can be reasoned by the range of curvature radius investigated. In Refs. [15] and [18], the small curvature radii were not considered (i.e. curvature radius was kept above 37 mm). Whereas, in the current study, this omission was rectified by taking small curvature radii into account (i.e. curvature radius ranged from 7 mm to 70 mm).

Fig. 3(b) shows the plot of maximum wall angle drawn against the half-side length of VWAPF. Up to 28 mm, the maximum wall angle increases, at a varying rate, with an increase in the half-side length. After 28 mm, the maximum wall angle becomes insensitive to any increase in the half-side length. These formability results are in good agreement with the wall thinning results shown in Fig. 3(a). In the investigated range, total increase in the maximum wall angle is approximately 3%. Therefore, the influence of change in the half-side length upon the formability of VWAPF should be considered while standardizing the test specimen.

Comparison between the formability of VWAPF and VWACF can be seen from Fig. 3(a). For small geometry sizes (i.e. curvature radii and half-side lengths below 37 mm), the VWAPF shows higher formability than VWACF, contrary to Capece et al. [18]. Contrarily, for large sizes (i.e. greater than 37 mm) the trend becomes reverse. Again, these trends can be attributed to the interesting patterns of wall thinning observed in Fig. 3(a). More in detail, for the size below 37 mm, the VWACF owing to higher wall thinning (as can be seen in Fig. 3(a)) and consequently achieving thinning limit at a smaller wall angle fractures earlier than VWAPF, and a converse trend occurs when the geometry size is above 37 mm.

The increase in the formability of VWACF test, under the same testing conditions, is about 5.5%, whereas that of VWAPF test is about 3%, thus revealing that the curvature radius is more influential upon the formability than the half-side length. This is worth noticing that the critical half-side length (i.e. the size further reduction in which adversely affects the formability) for VWAPF is about 50% smaller than that for VWACF. Moreover, the size of VWAPF and VWACF in horizontal plane should be kept above 28 mm and 54 mm, respectively, in order to achieve the maximum formability.

6.2 Effect of variation in initial forming angle

Fig. 4 shows the wall thinning, measured corresponding to 66.5° above fracture, of VWAPF with respect to varying initial forming angle. The wall thinning, despite no change in the half-side length[1] of test geometry, increases with increase in the initial forming angle. Total increase in wall thinning, within the investigated range, is about 5.5%. This is due to the occurrence of thinning band, as a result excessive thinning of sheet takes place and the Sine law fails to predict wall thickness (see an example of thinning band in Fig. 4 and Ref. [17] for further details). This is important to notice from Fig. 4 that the severity of thinning band on wall thinning increases as the initial forming angle increases. Further, the thinning band occurs when an initial forming angle larger than 51° is imposed.

The strain components, measured corresponding to 66.5° above fracture (these are not limiting strains), at two extreme settings are also shown in Fig. 4. The sum of components in VWAPF increases from 103% to 106% as the initial forming angle increases from 48° to 61°. This finding, which is an outcome of increasing the severity of thinning band with an increase in the initial forming angle, reinforces the finding that the variation in initial forming angle affects sheet deformation.

This is worth seeing from the photographs shown in Fig. 4, the fracture location in VWAPF shifts from the corner zone to the planar side as the initial forming (or wall) angle increases from 48° to 61°. *Prior to going into explanation, the reader may note down that the thinning band occurs, as found earlier, only when the value of initial forming angle exceeds 52°*. Also, the forthcoming points are not applicable to the findings reported in the preceding section. The reason behind fracture shifting is explained as follows:

[1] The half-side length was kept above critical value (i.e. 28 mm) so as to avoid adverse effect of smaller half-side length on fracture occurrence (Table 1).

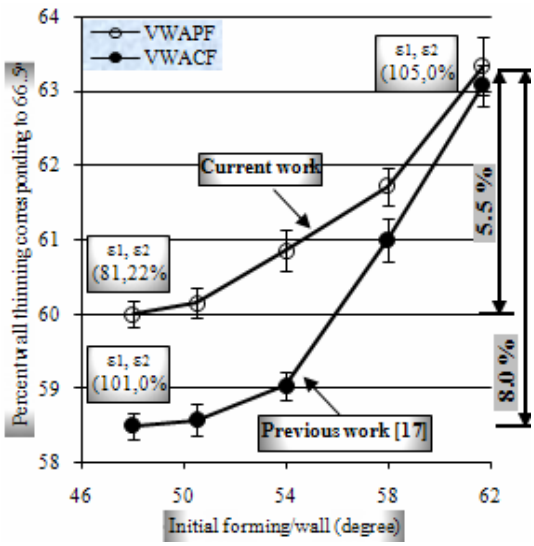

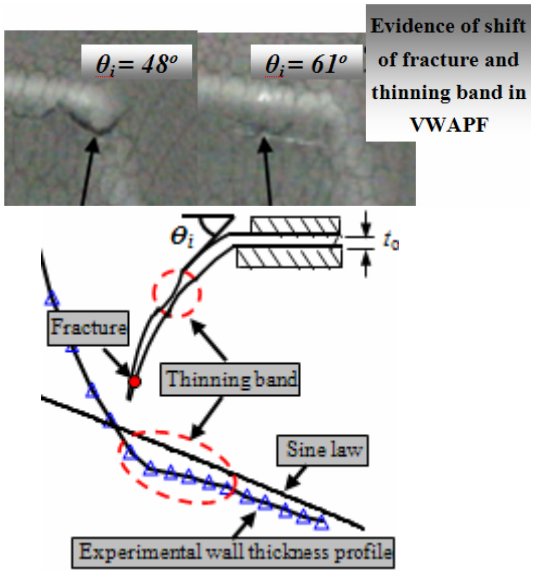

Fig. 4. Effect of variation in initial forming/wall angle upon wall thinning.

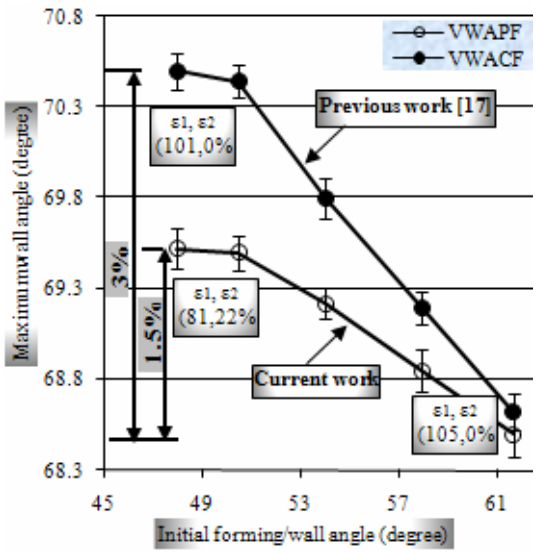

Fig. 5. Effect of variation in initial forming/wall angle upon formability.

• A point on the planar side of VWAPF subtends higher wall angle than the corresponding point on corner. Say the planar side subtends 61°; the corresponding corner (according to Eq. (3)) will subtend 52°.

• Due to the above difference in wall angle, the planar side faces higher severity of thinning band (i.e. higher wall thinning) than the corner. Further, this severity on planar side, compared to that on corner, increases as the initial forming angle increases, especially after 52° (minimum value of initial forming angle required for occurrence of thinning).

• Because of the above two points, the level of thinning (e.g. 63.2% at 61°) induced in the planar side becomes higher than the level of thinning (e.g. 62.2% at 61°) induced at corner (which normally experiences higher thinning when initial forming/wall angle is below 52°). Consequently the sheet fracture occurs at the planar side instead at the corner. Thus the strain mode at fracture also changes from bi-axial to uni-axial (compare strain states of VWAPF at two extreme settings in Fig. 4).

This is worth pointing out that such a condition happens only when a very large value of initial forming angle (such as 61°) is imposed. These findings clarify that the sheet fracture in a pyramid, contrary to Refs. [15, 18], does not necessarily occur at the corner zone rather the outcome depends upon the value of initial forming angle imposed.

Fig. 4 also portrays a comparison between the wall thinning of VWAPF and VWACF. It is to be seen that the wall thinning of former geometry approaches that of the latter one as the initial forming angle increases from 48° to 61°. This can be attributed to higher severity of thinning band on the planar side than on the corner, as discussed above in three points. The total variation in wall thinning, over the investigated range, in VWAPF is 5.5% and that in VWACF is 8%.

Fig. 5 depicts the effect of variation in the initial forming angle upon the formability (i.e. θ_{max}) of VWAPF. For the initial forming angle ranging from 48° to 51°, the formability remains un-affected. The formability sharply falls down as the initial forming angle increases from 51° to onwards. The overall reduction in the formability, in the investigated range, is about 1.5%. This result again can be attributed to undue thinning induced by thinning band, which causes premature sheet failure at a smaller angle and reduces formability.

The formability of VWAPF against that of VWACF can be compared from Fig. 5. The reduction in the formability of VWAPF is about 1.5%, whereas that in the formability of VWACF is about 2%. This means that the initial forming angle is relatively more influential upon VWACF than upon VAWPF. This is to be seen from the figure, the critical value of initial forming angle (i.e. the angle further increase in

Table 2. Sheet materials and their mechanical properties employed in this study.

Material	Tensile elongation (%)	Hardening exponent	Reduction in area at tensile fracture (%)
AA2024T4	19.34	0.171	24.75
AA2024O	21	0.236	41.53
Cu -H28	4.47	0.077	47
AA1060-H24	5.53	0.0427	70.45
AA-1060O	36.11	0.1968	81.5

which adversely affects sheet fracture) is about 51° for both the geometries. Furthermore, at smaller wall angles (say 48°) the formability of VWACF is larger than that of VWAPF. However, difference between the formability of two geometries (i.e. θ_{VWAPF} - θ_{VWACF}) gradually reduces as the initial forming angle increases till both the geometries, again in contrast to Capece et al. [18], show almost same formability at 61°. This finding is in good agreement with the one found regarding wall thinning discussed earlier.

7. Effect of variation in sheet material upon the formability

In Refs. [21], an analysis regarding formability-property relation in SPIF was conducted. The material properties were determined from tension test, and the formability in SPIF was evaluated making use of VWACF as test geometry. The geometrical parameters were chosen in such a way that neither biaxial deformation nor thinning band occurred during forming. The formability was found to be increasing with increase in percent reduction in area at tensile fracture (a material property). Here this result will be verified by changing the test geometry from VWACF to VWAPF. Furthermore, as found in the previous section, the difference between the formability of VWACF and VWAPF, i.e. $\theta_{max\ (VWACF)}$ - $\theta_{max\ (VWACF)}$, varies as the respective geometrical parameters are changed. This difference at varying sheet material is investigated in the current section. The formability of VWAPF geometry was obtained performing tests with five different materials, as listed in Table 2. Moreover, the geometry size was chosen comparable to that of VWACF. The strains were measured around fracture. The formability of VWACF and tensile properties of materials were adopted from Refs. [21]

Fig. 6 shows the correlation between the formability and percent reduction in area at tensile fracture. It can be seen that the formability, as expected, increases with the increasing of percent reduction in area and can be reasoned by the same fact as reported in Refs. [21]. The VWAPF, however, shows lower increase rate than VWACF. These findings reveal that the conclusion drawn in Refs. [21] regarding formability-property relation is equally valid for a pyramid as well.

The difference in the formability of two geometries, i.e. $\theta_{max\ (VWACF)}$ - $\theta_{max\ (VWAPF)}$, is also apparent from Fig. 6. The difference varies with variation in sheet material. It, as found for formability, increases from 3.5% to 8.5% as the percent reduction in area increases from 25% to 82%. This result can be attributed to increase in the development of hoop strains (from 7% to 34%) in VWAPF with increase in percent reduction in area (from 15% to 82%) (see Fig. 6). In fact, sheets with higher percent reduction in area can withstand larger wall angles (as can be seen from Fig. 6) without fracturing (i.e. from 50° to 74° in the investigated range). And, as evident from Eq. (3), at a large wall angle the forming tool makes a large contact with sheet (i.e. a large value of *r'* as defined in Fig. 2). Since, within the investigated range of percent reduction in area, the wall angle achieved by various materials varies from 50° to 74°, the value of *r'* in turn increases from 1.7 mm to 3.9 mm. As a result, due to increase in tool/sheet contact in hoop direction in addition to longitudinal one at the corner of VWAPF, the quantity of hoop strains (strains in this section were measured around fracture at the corner) at the corner in VWAPF increases (i.e. from 7% to 34%). On contrary, the VWACF owing to large curvature radius does not make significant contact in hoop direction and, therefore, does not undergo any hoop deformation (i.e. $\varepsilon_2 = 0$) (see Fig. 6). Due to these reasons, the difference between the sum of strain components in the two geometries increases as the percent reduction in area increases (compare strains sum at extreme settings). This increasing difference is strains sum consequently increases formability difference between the two geometries.

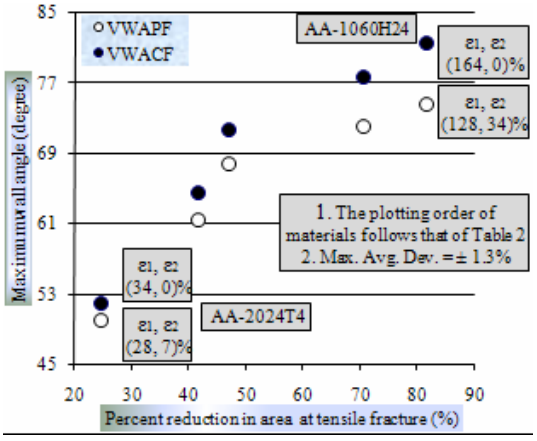

Fig. 6. Formability of test geometries at varying sheet material.

8. Conclusions

With an objective to standardize the test specimen in order to evaluate the formability with a single specimen during SPIF, the frustums of cone (i.e. VWACF) and pyramid (i.e. VWAPF) with wall angle continuously varying along the depth were compared in detail. The important findings of the study, which can act as guidelines to standardize the test specimen in SPIF, are as follows:

(1) For the two geometries, the formability shows a depend-

ence upon the size in horizontal plane (i.e. half-side length/curvature radius) of geometry. A pyramid, contrary to [15, 18], does not essentially show lower formability than a cone rather the outcome depends upon the size in horizontal plane.

(2) The critical size in horizontal plane for VWAPF is about 50% lesser than that for VWACF. To maximize the formability in SPIF, the geometry size should be kept larger than this critical size (i.e. above 28 mm for VWAPF and 54 mm for VWACF).

(3) The critical value of initial forming angle is same in both the geometries (i.e. 51^o). In order to achieve maximum formability, the initial forming angle should be kept below this critical value.

(4) The fracture in a pyramid, in contrast to Ref. [18], does not necessarily occur at the interface of corner and planar side. The fracture occurs at the interfacial zone if initial forming angle below 61^o is opted and at the planar side if initial forming angle above 61^o is imposed.

(5) The difference in the formability of VWACF and VWAPF (i.e. $\theta_{VWACF} - \theta_{VWAPF}$) depends upon the percent reduction in area at tensile fracture. This difference increases (from 3.5% to 8.5%) with an increase in the said material property. This finding will be helpful in clarifying the process mechanics.

9. Future work

The applicability of above findings on other materials of interest will be investigated in future.

Nomenclature

ρ_i : Initial curvature radius of VWACF in the horizontal plane
ρ_f : Final curvature radius of VWACF in horizontal plane
L_i : Initial half-side length of VWAPF in horizontal plane
L_f : Final half-side length of VWAPF in horizontal plane
θ : Wall angle subtended by planar wall of VWAPF
θ' : Wall angle subtended by corner wall of pyramid
θ_i : Initial forming/wall angle
θ_f : Final wall angle
ε_1 : Longitudinal strain
ε_2 : Hoop strain
h : Depth of specimen
R : Generatrix radius
r : Tool radius
r' : Effective tool radius

References

[1] R. M. N. Jorge, R. A. F. Valente, A. P. Roque, M. P. Parente and A. A. Fernandes, Numerical simulation of hydro-forming process involving a tubular blank with dissimilar thickness, *Materials and Manufacturing Processes,* 22 (2007) 286-291.

[2] Z. Yong, L. C. Chan, W. Chunguang and W. Pei, Optimization for loading paths of tube hydro-forming using a hybrid method, *Materials and Manufacturing Processes*, 24 (2009) 700-708.

[3] G. H. Faraji, R. Hashemi, R. M. Mashhadi, A. F. Dizaji and V. Norouzifard, Hydro-forming limits in metal bellows forming process, *Materials and Manufacturing Processes*, 25 (2010) 1413-1417.

[4] J. Laeng, J. G. Stewart and F. W. Liou, Laser metal forming processes for rapid prototyping - A review, *International Journal of Production Research*, 38 (200) 3973-3996.

[5] B. Jurisevic, K. Kuzman and K. Junkar, Water jetting technology: an alternative in incremental sheet metal forming, *International Journal of Advanced Manufacturing Technology*, 31(2006) 18-23.

[6] H. S. Chan, Y. H. Seo, T. Ku and B. S. Kang, Formability evaluation of dimple forming process based on numerical and experimental approach, *Journal of Mechanical Science and Technology*, 25 (2011) 429-439.

[7] S. C. Heo, Y. H. Seo, J. W. Park, T. W. Ku, J. Kim and B. S Kang, Application of flexible forming process to hull structure forming, *Journal of Mechanical Science and Technology*, 24 (2010) 137-140.

[8] J. Jeswiet, F. Micari, G. Hirt, A. Bramley, J. Duflou and J. Allwood, Asymmetric single point incremental forming of sheet metal, *CIRP Annals*, 54 (2005) 623-650.

[9] H. Amino,Y. Lu, S. Ozawa, K. Fukuda and T. Maki, Dieless NC forming of automotive service panels, *Proc. of the Conference on Advanced Techniques of Plasticity*, (2002) 1015-1020.

[10] K. Jackson, J. Allwood and M. Landert, Incremental forming of sandwich panels, *Proc. of International Conference on Sheet Metal, Palermo, Sicily*, (2007) 591-598.

[11] G. Ambrogio, L. De. Napoli, L. Filice, F. Gagliardi and M. Muzzupappa, Application of incremental forming process for high customized medical product manufacturing, *Journal of Materials Processing Technology*, 162-163 (2005) 156-162.

[12] H. Takano, K. Kitazawa and T. Goto, Incremental forming of non-uniform sheet metal: Possibility of cold recycling process of sheet metal waste, *Journal of Materials Processing Technology,* 48 (2008) 477-482.

[13] V. Franzen, L. Kwiatkowski, P. A. F. Martins and A. E. Tekkayaa, Single point incremental forming of PVC, *Journal of Materials Processing Technology*, 209 (2008) 462-469.

[14] K. Jackson and J. Allwood, The mechanics of incremental sheet forming, *Journal of Materials Processing Technology*, 209 (2008) 1158-1174.

[15] M. S. Shim and J. J. Park, The formability of aluminum sheet in incremental forming, *Journal of Materials Processing Technology*, 113 (2001) 654-658.

[16] G. Hussain, L. Gao, N. Hayat and A. Iqbal, On the effect of curvature radius on spif-ability, *Advanced Materials Re-*

search, 129-131 (2009) 1222-1227.

[17] G. Hussain, N. Hayat and L. Gao, An experimental study on the effect of thinning band on the sheet formability in negative incremental forming, *International Journal of Machine Tools and Manufacture*, 48 (2008) 1170-1178.

[18] M. F. Capece, M. Durante, A. Formisabo and A. Langella, Evaluation of the maximum slope angle of simple geometries carried out by incremental forming process, *Journal of Materials Processing Technology*, 194 (2007) 145-150.

[19] G. Hussain, L. Gao, N. Hayat and L. Qijian, The effect of variation in the curvature of part on the formability in incremental forming: An experimental investigation. *International Journal of Machine Tools and Manufacture*, 47 (2007) 2177-2181.

[20] G. Hussain, L. Gao and N. Hayat, A new parameter and its effect on the formability in single point incremental forming: a fundamental investigation, *Journal of Mechanical Science and Technology*, 24 (2007) 1-7.

[21] G. Hussain, N. Hayat, L. Gao and Xu Ziran, A new formability indicator in single point incremental forming, *Journal of Materials Processing Technology*, 209 (2009) 4237-4242.

Ghulam Hussain in August 2000, completed his undergraduate studies in Mechanical Engineering from UET Lahore, Pakistan. Later, after four years working in a manufacturing industry, he completed his Ph.D in manufacturing engineering from Nanjing University of Aeronautics & Astronautics, P.R China, in March 2009. Presently, the author is working on novel metal forming processes.